
Graph-based Unsupervised Disentangled Representation Learning via Multimodal Large Language Models

Baao Xie¹ Qiuyu Chen^{1,2} Yunnan Wang^{1,2} Zequn Zhang¹ Xin Jin^{1,*} Wenjun Zeng¹

¹Ningbo Institute of Digital Twin, Eastern Institute of Technology, Ningbo, China

² Shanghai Jiao Tong University, Shanghai, China

*Corresponding: jinxin@eitech.edu.cn

Abstract

Disentangled representation learning (DRL) aims to identify and decompose underlying factors behind observations, thus facilitating data perception and generation. However, current DRL approaches often rely on the unrealistic assumption that semantic factors are statistically independent. In reality, these factors may exhibit correlations, which off-the-shelf solutions have yet to properly address. To tackle this challenge, we introduce a bidirectional weighted graph-based framework, to learn factorized attributes and their interrelations within complex data. Specifically, we propose a β -VAE based module to extract factors as the initial nodes of the graph, and leverage the multimodal large language model (MLLM) to discover and rank latent correlations, thereby updating the weighted edges. By integrating these complementary modules, our model successfully achieves fine-grained, practical and unsupervised disentanglement. Experiments demonstrate our method's superior performance in disentanglement and reconstruction. Furthermore, the model inherits enhanced interpretability and generalizability from MLLMs.

1 Introduction

Disentangled representation learning (DRL) is a major goal of artificial intelligence (AI), acclaimed for its enhancement of model robustness, interpretability, and generalizability. Essentially, DRL methods imitate the understanding processes of biological intelligence, wherein comprehension of real-world is achieved by separating observations into distinct factors [1]. In this form, specific attributes (e.g., object color, shape, and size) exhibit exclusive sensitivity to the changes of specific factors. Learning of such disentangled representations is of great importance across various domains, e.g., computer vision [2, 3, 4, 5], natural language processing [6, 7, 8], and AI generated content [9, 10, 11]. In the current phase, unsupervised DRL methods primarily utilize the Variational Autoencoder (VAE) framework [12], a probabilistic model learning representations through a regularization term. This term involves the Kullback-Leibler divergence between the posterior distribution of latent factors and a standard multivariate Gaussian prior, thereby encouraging the factorized representations. To strengthen disentanglement, co-current research [13, 14, 15, 16] focus on the optimization and refinement of the original VAE regularizers, resulting in the family of VAE-based DRL approaches.

Despite the advanced results of the simple and synthetic datasets, VAE-based DRL methods still fall short in interpretability and robustness that are required for effective disentanglement in complex data [17]. This limitation mainly stems from the unrealistic assumption that underlying factors are countable, independent, and can be fully disentangled in an unsupervised manner (refer to the top-left of Figure 1). In contrast, the real-world variables are pervasively correlated: red apples are more common than yellow ones; elderly people are more frequent with white hair and a receding

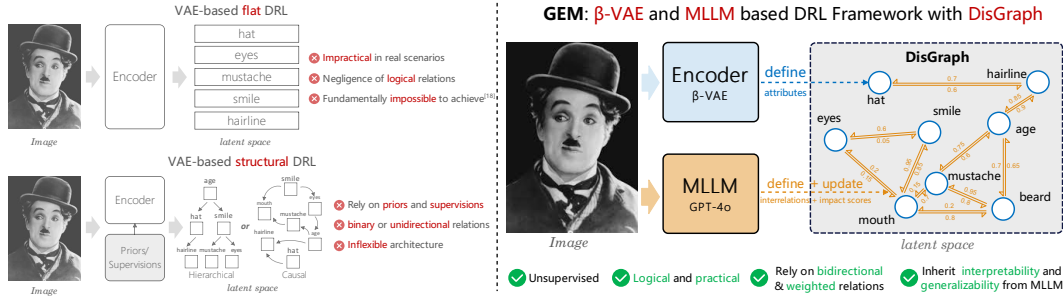


Figure 1: The comparison of typical DRL frameworks with our GEM. The limitations of conventional DRL methods are presented on the left. Conversely, the right-hand side illustrates the advantages of our framework, which benefited from the integration of the β -VAE and MLLMs.

hairline. Accordingly, an increasing number of recent studies [18, 19, 17, 20] showcases that purely unsupervised DRL is fundamentally impossible without extra priors and inductive biases.

The struggle of typical DRL methods on the complex data returns us back to the essential goal of DRL, i.e., understanding the world as biological intelligence does. This cognitive process can be naturally segmented into three phases: attribute extraction, interrelation perception, and knowledge combination [21, 22], where the latter two stages should not be neglected. From this perspective, several structured DRL approaches, typically known as Hierarchical DRL [23, 24, 11] and Causal DRL [19, 25, 26, 27], have involved the correlations between attributes. However, these approaches usually require extra supervision, and their relations are invariably represented by binary and unidirectional fusion, thus limiting the model performance in practical scenarios (refer to the bottom-left of Figure 1). Inspired by the analysis above, we argue that an effective and practical disentanglement framework should meet the following criteria: (i) the framework should be fully unsupervised; (ii) the framework should be able to disentangle factors while concurrently discovering logical interrelations among them; (iii) the interrelations should be modeled as bidirectional, with corresponding impact scores assigned to each, thereby improving model performance in complex scenarios. On this basis, we propose a novel Graph-based disEntanglement framework with Multimodal large language models, dubbed **GEM**. Specifically, our model employs two complementary branches: a β -VAE based disentanglement branch for the attribute extraction, and a multimodal large language model (MLLM) based branch for the interrelation discovery. The relation-aware representations are further embedded into a disentangled bidirectional weighted graph (DisGraph), which presents distinct factors as nodes, interrelations as edges, and impact scores as weights. The parameters of the graph are dynamically updated and refined via a graph learner. The experimental results show that GEM achieves superior performance on fine-grained and relation-aware disentanglement, while preserving the reconstruction quality. Furthermore, the model is endowed with superior interpretability and generalizability that derived from MLLMs. All in all, our main contributions can be summarised as:

- To our best knowledge, we are the first to leverage the commonsense reasoning of MLLMs to discover and rank the semantic interrelations from the perspective of DRL.
- We propose a novel and practical disentanglement framework built upon β -VAE and MLLMs to learn the independent factors and their interrelations in an unsupervised way.
- We introduce a bidirectional and self-driven graph architecture to encode the relation-aware representations, thus facilitating practical and controllable disentanglement.

2 Related Work

2.1 Standard Disentangled Representation Learning

The definition of DRL is intuitively given by Bengio et al. [1] as a technique to separate semantic factors behind observational data. This approach assumes that individual data attributes are sensitive to changes in single latent factors, while not being affected by other factors. The disentanglement of attributes is believed helpful for downstream tasks, e.g., generative models [3, 28, 5, 29, 30], medical imaging [31, 32, 33], image editing [34, 35, 36, 37], and 3D reconstruction [38, 39, 40].

Traditional DRL methods primarily utilize the VAE framework, achieving a measure of disentanglement on static datasets. This framework has been further enhanced by extensive models such as β -VAE [13], β -TCVAE [14], DIP-VAE [4], FactorVAE [41], RF-VAE [42], and α -TCVAE [16] through the optimizations of regularization terms. Despite the successes on simple and static datasets, standard DRL approaches still encounter challenges in complex data. It is mainly due to the flat and unrealistic assumption: data properties are independent and can be factorized into distinct factors [1, 19, 43, 44]. Locatello et al. [18] have proven that unsupervised DRL is fundamentally impossible without extra priors. Thus, subsequent studies have demonstrated that a practical DRL model with appropriate inductive biases can enhance the disentanglement in real scenes [45, 46, 47, 48].

2.2 Structured Disentangled Representation Learning

In contrast to the flat and VAE-based DRL methods, recent research gradually realizes that latent factors might naturally involve semantic interrelations, deriving to the branch of structured disentangled representation learning [17]. Within this domain, Hierarchical DRL and Causal DRL are mostly relevant to our work. Hierarchical DRL presumes that underlying factors have different levels of semantic abstraction, either dependent [49] or independent [23] across levels. While straightforward, Li et al. [23] propose a hierarchical VAE-based model to learn semantic representations. Furthermore, Singh et al. [11] introduce FineGAN, a three-tier hierarchical framework for controllable object generation. Li et al. [50] also propose a hierarchical DRL framework aimed at facilitating image-to-image translation. Differently, our framework aims to achieve fine-grained disentanglement, where the targeted attributes are always flat, e.g., the wrinkle, lipstick, and mustache of faces. Therefore, we rely on the flat representations, but place a strong emphasis on the mutual relations between attributes.

Similarly, Causal DRL methods endeavor to capture the causal relations between disentangled factors. As the first, Yang et al. [19] propose CausalVAE to discover relations from the perspective of causality. Further, Shen et al. [27] propose a weakly supervised framework DEAR with the structured causal model (SCM) as prior. However, in our view, current Causal DRL methods have at least three unpractical issues: (i) rely on various degrees of supervision; (ii) aim to model a specific event rather than a common scenario; (iii) the causal relationship is often overly simplistic, being impractically binary and unidirectional, i.e., paired variables A and B only have two possible causal relations: either $A \rightarrow B$ or $A \leftarrow B$ (otherwise unrelated). In practical, it is common for paired variables to exhibit bidirectional influence, and the impact of such bidirectional relations should be properly ranked.

2.3 Multimodal Large Language Models

Recent years have witnessed the remarkable advancements in Multimodal Large Language Model (MLLM) [51, 52, 53, 54]. Since the release of Generative Pre-trained Transformer (GPT) [55], there has been a research trend over MLLMs regarding to its demonstrated potential in processing multimodal data [56, 57, 58]. As the variants of GPT-4, GPT-4 with Vision (GPT-4V) [59] and GPT-4 omni (GPT-4o) [60] enhance to process textual and visual data, enabling richer, context-aware interactions across a range of multimodalities. Concurrently, following works such as Gemini [56], Claude [61], NExT-GPTs [62] and GLM-4 [63] have strengthened the support to additional modalities.

The powerful capacities of MLLMs gradually make researchers aware of its latent perceptual knowledge embedded within networks. Gandelsman et al. [57] investigate the way that CLIP encoder understands visual data, by decomposing representations into individual components. In addition, Basu et al. [64] propose a mechanistic localization approach to explore how the visual properties are encoded in MLLMs. However, to our best knowledge, there is limited exploration into leveraging the commonsense reasoning of MLLMs from the perspective of DRL. And we are the first to employ MLLMs to discover and rank interrelations between semantic factors in the DRL framework.

3 Methodology

To achieve fine-grained and relation-aware disentanglement, we propose GEM, a novel and practical framework that synergizes the strengths of DRL and MLLMs by a bidirectional weighted DisGraph. As depicted in Figure 2, GEM is comprised of two complementary modules: a β -VAE based branch dedicated to extract attributes (Section 3.1), and a MLLM-based branch to discover and rank

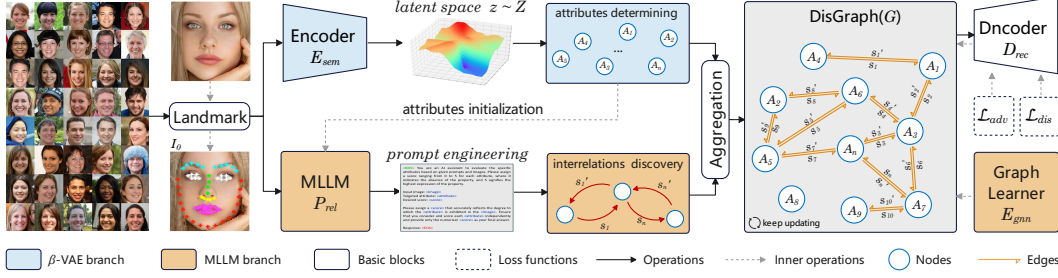


Figure 2: Pipeline of our GEM. The model consists of two complementary branches, termed as a β -VAE branch (blue) and a MLLM branch (brown). The former utilizes β -VAE based semantic encoder E_{sem} to disentangle underlying factors, while the latter employs prompt engineering to discover and rank interrelations. The bidirectional weighted DisGraph G is further proposed to embed relation-aware representations, with its parameters optimized constantly by a GNN network E_{gnn} .

interrelations (Section 3.2). The relation-aware representations are then embedded into the DisGraph (Section 3.3), which presents factors as nodes, interrelations as edges, and impact scores as weights.

3.1 Beta-VAE based Attribute Determining Branch

The fundamental objective of vanilla VAE is to approximate data distributions by employing a maximum likelihood estimation framework as outlined in Eq. 1:

$$\log p_{\theta}(\mathbf{x}) = D_{KL}(q_{\phi}(\mathbf{z}|\mathbf{x})||p_{\theta}(\mathbf{z}|\mathbf{x})) + \mathcal{L}(\theta, \phi) \quad (1)$$

where the variational posterior distribution $q_{\phi}(\mathbf{z}|\mathbf{x})$ is utilized to represent the probability distribution of the latent variable z given the observation x . The key of Eq. 1 is maximizing the approximation $\log p_{\theta}(\mathbf{x})$ of the true posterior distribution $p_{\phi}(\mathbf{z}|\mathbf{x})$ and $q_{\phi}(\mathbf{z}|\mathbf{x})$.

Specifically, the first term of Eq. 2 corresponds to the Kullback-Leibler (KL) divergence measuring the distance between distribution $q_{\phi}(\mathbf{z}|\mathbf{x})$ and $p_{\theta}(\mathbf{z}|\mathbf{x})$. The second term is denoted as the variational evidence lower bound (ELBO). Empirically, the maximization of ELBO is employed to provide a stringent tight lower bound for the original log-likelihood $\log p_{\theta}(\mathbf{x})$. ELBO can be reformulated as:

$$\mathcal{L}(\theta, \phi) = \mathbb{E}_{q_{\phi}(\mathbf{z}|\mathbf{x})} [\log p_{\theta}(\mathbf{x}|\mathbf{z})] - \beta D_{KL}(q_{\phi}(\mathbf{z}|\mathbf{x})||p_{\theta}(\mathbf{z})) \quad (2)$$

where the initial term, i.e., conditional logarithmic likelihood $\mathbb{E}_{q_{\phi}(\mathbf{z}|\mathbf{x})} [\log p_{\theta}(\mathbf{x}|\mathbf{z})]$ is responsible for the reconstruction. Typically, the latent variable z is assumed to follow a standard Gaussian distribution $\mathcal{N}(0, 1)$ for $p_{\theta}(z)$, so that the KL term actually imposes independent constraints on the representations. Furthermore, subsequent studies [13, 15, 65] highlight that a extra penalty coefficient prior to the KL term, denoted by β , can significantly strengthen disentanglement. When β is set to 1, the β -VAE reverts to the standard VAE framework. And an increase in β encourages more disentangled representations but harms the performance of reconstruction as a trade-off.

As shown in Figure 2, the input image is firstly subjected to a pre-processing step utilizing landmark detection functions as instructed by [66] and [67]. It serves as a regularization phase, to remain the key features through targeted cropping. The supplementary results of this step can be found in the appendix. Then, the pre-processed I_0 is fed into a β -VAE based branch, designed to disentangle factors associated with each dimension in the latent variable $z \in Z$. However, the input of decoder D_{rec} is the relation-aware variable $z_{rel} = \mathbf{A}^T z$ from the DisGraph, rather than the $z \in Z$. It means the prior assumption of $p_{\theta}(z) \in \mathcal{N}(0, 1)$ is no longer hold. To address this issue, we reformulate the loss function in β -VAE as follows:

$$\nabla_{\theta} \mathcal{L}(\theta, \phi) \stackrel{x=D_{rec}^{\theta}(z)}{=} \mathbb{E}_{z \sim q(z)} \nabla_x \left[\log \left(\frac{p_{\theta}(x, z)}{\beta q_{\phi}(x, z)} \right) \right] \nabla_{\theta} x + \beta \mathbb{E}_{z \sim q(z)} \nabla_x q_{\phi}(x) \nabla_{\theta} x \quad (3)$$

$$\nabla_{\phi} \mathcal{L}(\theta, \phi) \stackrel{z=E_{sem}^{\phi}(x)}{=} \mathbb{E}_{x \sim p(x)} \nabla_z \left[\log \left(\frac{p_{\theta}(x, z)}{\beta q_{\phi}(x, z)} \right) \right] \nabla_{\phi} z + \beta \mathbb{E}_{x \sim p(x)} \nabla_z q_{\phi}(x) \nabla_{\phi} z \quad (4)$$

where the ϕ and θ are the learnable parameters of E_{sem} and D_{rec} , respectively. The second term responds to disentanglement, whereas the first term addresses reconstruction, which necessitates an

extra neural network to fit. Let’s say $D(x, y) = \log\left(\frac{p_\theta(x, z)}{\beta q_\phi(x, z)}\right)$, and the the gradients with respect to x and z can be obtained during backpropagation by the cross-entropy:

$$\mathcal{L}_{adv} = \mathcal{L}_{D(x, y)} = \frac{1}{N_{bc}N_m} \left[\sum_{i=0}^{N_{bc}} \text{softplus}(-D(x_i, z_i)) + \sum_{i=0}^{N_{bc}} \text{softplus}(D(x_i, z_i)) \right] \quad (5)$$

where N_{bc} and N_m represent the number of samples and the posterior samples in a batch, respectively. Obviously, this loss resembles the adversarial loss utilized in Generative Adversarial Networks (GAN) [68]. Therefore, we employ the adversarial training strategy to optimize $D(x, y)$. Combined with the disentanglement term from the original β -VAE indicated as \mathcal{L}_{dis} , the total loss for the attribute determining branch can be expressed as:

$$\mathcal{L}_{total} = \lambda_{adv}\mathcal{L}_{adv} + \lambda_{dis}\mathcal{L}_{dis} \quad (6)$$

where the λ_{adv} and λ_{dis} serve as hyperparameters to balance the disentanglement capability and reconstruction quality, with default values set to 0.8 and 0.6, respectively. The detailed derivation process of the adversarial training strategy is provided in the supplementary material.

3.2 MLLM-based Interrelation Discovery Branch

Given a pre-processed image I_0 with n targeted attributes $\mathcal{A} = \{1, 2, 3, \dots, n\}$ initialized by the β -VAE branch, our objective is to discover and rank the mutual relations for each pair within \mathcal{A} . As represented by the brown blocks in Figure 2, we employ MLLMs as a relation predictor P_{rel} to discover and rank interrelations. Initially, the MLLM is required to score from 0 to 5 for each attribute, where 0 indicates the attribute’s absence, and 5 denotes its highest expression. As shown in Figure 3, the queries can be formulated as a question in natural language with the input image I_0 .

Based on the attribute scores, we subsequently employ Somers’ D algorithm [69] to rank the bidirectional impact scores of interrelations. For the attribute pair (A_i, A_j) , we determine the number of concordant pairs N_C and discordant pairs N_D , as delineated by Kendall’s Tau [70]. Subsequently, the impact score S_{ij} within $\mathcal{S} = \{1, 2, 3, \dots, k\}$ can be denoted as:

$$S_{ij} = \frac{N_c - N_d}{N_c + N_d + T_i} \quad (7)$$

For the reversed relation of (A_i, A_j) , the impact score can be denoted as S_{ji} or S'_{ij} :

$$S'_{ij} = S_{ji} = \frac{N_c - N_d}{N_c + N_d + T_j} \quad (8)$$

where T_i and T_j is the number of ties only for the independent variable A_i and A_j , respectively. The calculated \mathcal{S} and \mathcal{S}' are used for initialization and refinement of DisGraph (see Section 3.3). To ascertain the reliability of MLLMs for interrelation discovery, extra experiments are performed as shown in Section 4.4.

3.3 Bidirectional Weighted DisGraph

Based on the extracted factors and interrelations, we then propose the bidirectional weighted DisGraph $\mathcal{G} = (\mathcal{A}, \mathcal{E}, \mathcal{S})$ to integrate the semantic representations. Specifically, \mathcal{A} is the set of $n = |\mathcal{A}|$ nodes, embodying the disentangled attributes as factors. Besides, \mathcal{E} is the set of $k = |\mathcal{E}|$ edges, and \mathcal{S} stands for the weights of these edges. An $e \in \mathcal{E}$ and its corresponding impact score $s \in \mathcal{S}$ are embedded. Consequently, \mathcal{G} can be presented as the learnable weighted adjacency matrix $\mathbf{A} \in [0, 1]^{n \times n}$.

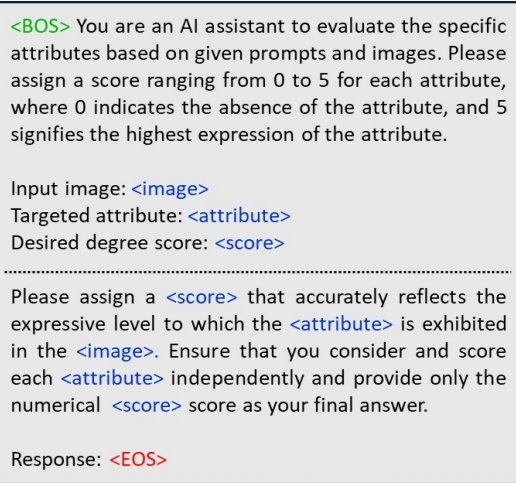


Figure 3: A simplified example of the template for prompting MLLMs to evaluate attributes. Specifically, `<text>` is the interactive token, while `<BOS>` and `<EOS>` are tokens denoting the start and end of the input to MLLMs, respectively.

According to the definitions above, the model firstly constructs a sketched adjacency matrix $\mathbf{A}_0 \in \mathbb{R}^{n \times n}$ upon the factors and relations initialized by the β -VAE branch and MLLM branch. Specifically, we treat the averaged impact scores of the first 1,500 images processed by MLLMs, as initial weights of relations. We further employ an unsupervised graph learner E_{gnn} [71, 72] to dynamically refine the parameters of DisGraph. The optimization function of E_{gnn} can be formulated as:

$$\mathbf{T}^{(l)} = h_w^{(l)}\left(\mathbf{T}^{(l-1)}, \mathbf{A}\right) = \sigma\left(\tilde{\mathbf{D}}^{-\frac{1}{2}} \tilde{\mathbf{A}} \tilde{\mathbf{D}}^{-\frac{1}{2}} \mathbf{T}^{(l-1)} \Omega^{(l)}\right) \quad (9)$$

It converts the sketched adjacency matrix \mathbf{A}_0 into node embedding \mathbf{T} via the GNN-based multilayer network, where $h_w^{(l)}(\cdot)$ is the embedding function with learnable parameters w of the l -th layer and $\mathbf{T}^{(l)}$ is the output matrix. The augmented adjacency matrix $\tilde{\mathbf{A}} = \mathbf{A} + \mathbf{I}$ incorporates self-loops based on the initial matrix \mathbf{A}_0 , and $\tilde{\mathbf{D}}$ is the degree matrix of \mathbf{A} . Further, $w^{(l)} = \Omega^{(l)} \in \mathbb{R}^{n \times n}$ denotes the parameter matrix of the l -th layer, with $\sigma(\cdot)$ as a non-linear function that enhances training stability.

4 Experiments

Datasets. We evaluate the GEM on two datasets: 1) **CelebA** [73] contains over 200,000 high-quality facial images. Each image is annotated with 40 binary attribute labels, making it a widely used benchmark for supervised DRL methodologies. Operating in an unsupervised manner, we do not utilize ground-truth labels from this dataset, yet we still conduct comparisons against the supervised approaches; 2) **LSUN** [74] consists of about one million images across various object categories such as cars, buildings, animals, etc. We select a typical subset from both scene categories and object categories, as bedroom and horse, respectively. We believe these two datasets are diverse enough to assess our method covering complex data of different object types.

Implementation details. We implement GEM with PyTorch [75]. The landmark pre-processing settings follow the instructions of [66] and [67]. In addition, we employ the latest GPT-4o [60] as the interrelation predictor. For every experiment, the latent dimension size is set to 6. Concentrating on the disentanglement capacity of the framework, all experimental images are resized to a resolution of 64×64 to minimize computational resources. For high-definition outcomes at 256×256 , refer to Appendix. All the experiments are processed using the Adam optimizer with a learning rate of $1e-4$, and conducted on the Nvidia Tesla A100 GPUs, with a batch size of 32.

Baselines for Comparison. We evaluate the GEM with state-of-the-art DRL methods on the disentanglement capacity, reconstruction quality, and computational efficiency. The comparison encompasses supervised and unsupervised models, including standard VAE [12], β -VAE [13], β -TCVAE [14], FactorVAE [41] and DEAR [27]. All baselines are trained using the complete CelebA dataset under the configurations previously specified.

4.1 Qualitative Results

To evaluate the GEM’s effectiveness of relation-aware and fine-grained disentanglement, we perform qualitative analyses with FactorVAE [41] and DEAR [27]. The experiments are conducted on CelebA, a standard benchmark that has been previously validated as compatible with these methods. We select the six fine-grained facial attributes from the database including *Bangs*, *Bald*, *Gender*, *Beard*, *Blond*, and *Makeup*. The disentanglement results are represented by traversals across various latent dimensions, where each dimension corresponds to distinct attributes.

As illustrated in Figure 4, GEM effectively achieves fine-grained and relation-aware disentanglement, via the integration of DRL and MLLMs. The interrelations determined by MLLMs are depicted as a heatmap in the bottom-right of Figure 4, where deeper colors reflect stronger relations. Since DisGraph is bidirectional, the impact scores for bidirectional relations between a pair of attributes may vary, resulting in an asymmetric matrix. Specifically, in the first row of GEM’s result, a person with heavier *Bangs* is less likely to be *Bald*, and the hair tends to be *Blond*, which is considered logical by MLLMs. Furthermore, as shown in the second and third rows, males (*Gender*) are more likely to be *Bald* and less likely to have *Blond* hair. The attribute *Makeup* is considered as relatively independent, with lower impacts scores among other attributes.

In comparison, DEAR demonstrates limitations in learning specific attributes such as *Bald* (second row) and *Gender* (third row), while the relations between attributes appear to be tenuous. To our

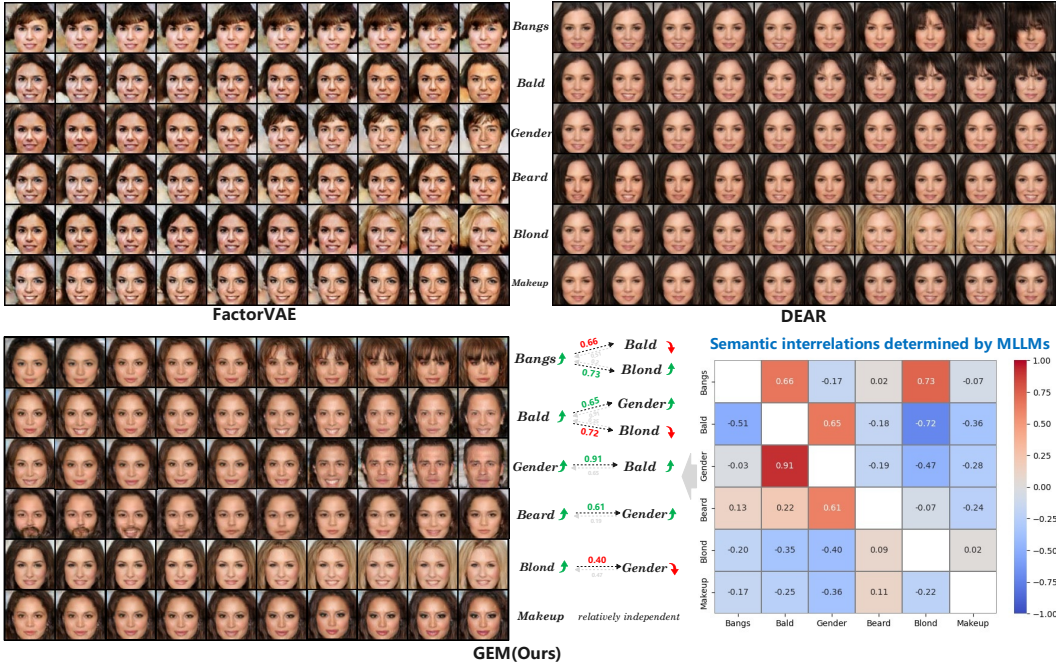


Figure 4: Qualitative comparisons between GEM and typical DRL Methods. Each row in facial images corresponds to the traversal results on a specific attribute, as indicated adjacent to the images (i.e. *Bangs*, *Bald*, *Gender*, *Beard*, *Blond*, and *Makeup*). GEM exhibits superior ability in fine-grained disentanglement with discovered practical and bidirectional relations (illustrated by the heatmap).

knowledge, this underperformance may stem from the stringent nature of causal relations, which are single-directional and heavily rely on the quality of prior. For FactorVAE, since it is a flat DRL framework, we employ the same causal relations used in DEAR to make it relation-aware. As shown in Figure 4, GEM surpasses FactorVAE in both attribute disentanglement and relation discovery, which indicates the importance of specially-designed modules within our framework.

4.2 Quantitative Results

Table 1 reports the results of Fréchet Inception Distance (FID) [68] and Kernel Inception Distance (KID) [68] scores to verify the quality of reconstructed images. To ensure statistical significance, each comparison model undergoes three rounds of evaluations in the same configuration. The results indicate that GEM outperforms both typical unsupervised (VAE, β -VAE, β -TCVAE, FactorVAE) and supervised approaches (DEAR) in terms of reconstruction quality. To our understanding, this superior performance is attributed to the specialized training strategy implemented in the framework.

Table 1: Quantitative comparison results with typical DRL approaches in FID and KID.

Method	CelebA		LSUN-horse		LSUN-bedroom	
	FID ↓	KID $\times 10^3$ ↓ ↑	FID ↓	KID $\times 10^3$ ↓	FID ↓	KID $\times 10^3$ ↓
VAE [13]	53.3 \pm 0.6	51.4 \pm 0.4	172.8 \pm 1.7	181.7 \pm 2.1	195.8 \pm 4.1	226.4 \pm 5.4
β -VAE [13]	136.2 \pm 1.6	107.0 \pm 2.7	272.4 \pm 3.2	294.2 \pm 5.3	288.1 \pm 5.7	225.7 \pm 6.0
β -TCVAE [14]	139.1 \pm 0.8	113.2 \pm 4.1	173.0 \pm 4.8	217.35 \pm 9.2	191.0 \pm 5.0	179.2 \pm 7.4
FactorVAE [41]	134.5 \pm 0.3	92.0 \pm 0.5	248.5 \pm 5.5	155.3 \pm 3.7	235.7 \pm 3.2	172.8 \pm 3.9
DEAR [27]	70.7 \pm 0.3	52.6 \pm 0.1	136.4 \pm 1.6	113.7 \pm 0.9	177.6 \pm 3.5	157.8 \pm 2.3
GEM (Ours)	46.0 \pm 0.1	48.3 \pm 0.2	101.0 \pm 1.1	65.5 \pm 1.7	125.4 \pm 1.2	76.1 \pm 1.1

As shown in Table 1, GEM surpasses baseline models in reconstruction quality on the datasets of CelebA, LSUN-horse, and LSUN-bedroom. However, the use of the disentanglement coefficient in the β -VAE branch leads to an inevitable trade-off in reconstruction quality, making the model less comparable to these generative models (e.g., GAN and Diffusion [76]). Therefore, the integration with powerful generative models can be a direction for our future work.

Furthermore, we evaluate four relation-aware models: FactorVAE, DEAR, GEM (Single), and GEM (Full), on quantitative comparisons of computational resources. Notably, GEM (Single) is the

Table 2: Computational efficiency report in parameters size, FLOPs, memory cost and training time.

Models	Params(M)	GFLOPs(B)	Mem(M)	TT(s)
FactorVAE	55.9	3.8	200.5	63.9
DEAR	53.4	3.5	267.2	91.8
GEM (Single)	44.7	2.8	173.6	51.5
GEM (Full)	49.6	3.2	222.8	78.9

variant of GEM that incorporates single attribute determination branch (we only provide the initial relations to make it relation-aware). Table 2 shows that GEM outperforms DEAR and is comparable to FactorVAE on computational efficiency. This is mainly attributed to FactorVAE’s utilization of a simple convolutional encoder, whereas GEM employs a β -VAE based encoder to strengthen disentanglement. In addition, the efficiency of full GEM is slightly inferior to GEM (Single), due to the extra modules for relation discovery and refinement.

4.3 Evaluations of Interpretability and Generalizability

As a by-product, GEM inherits the interpretability and generalizability of MLLMs. Theoretically, owing to the commonsense reasoning faculties of MLLMs, our model can be generalized to discover any attributes and interrelations across various real-world objects and scenes. To demonstrate the robustness and generalizability of GEM, we perform extra experiments on more complex scenes in LSUN, specifically targeting the typical object subset LSUN-horse and the scene subset LSUN-bedroom. Furthermore, we test the attributes beyond the 40 specified in CelebA, collectively showcasing the model’s superiority. To highlight the characteristics of bidirectional weighted DisGragh, we intentionally select paired fine-grained attributes exhibiting inconsistent bidirectional relations.

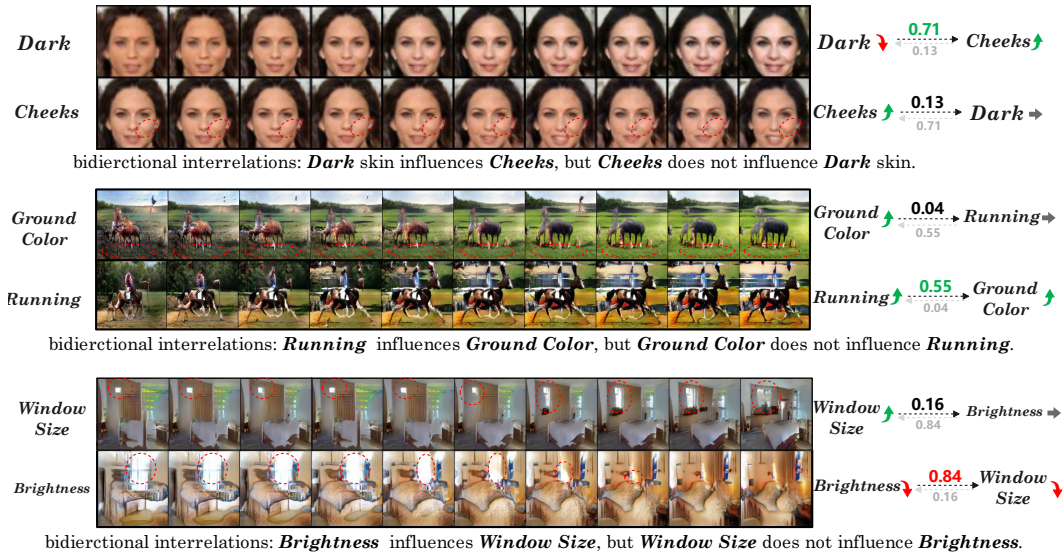


Figure 5: Relation-aware disentanglement results on LSUN and the attributes beyond CelebA. Paired fine-grained attributes with inconsistent bidirectional relations are chosen to indicate effectiveness.

As depicted in Figure 5, GEM successfully achieve fine-grained disentanglement on complex scenes, while identifying bidirectional and weighted relations among attributes. Furthermore, the artifacts observed in the results of LSUN datasets are mainly due to the datasets’ clutter (evidenced by the increase of FID and KID scores in Table 1). Nonetheless, despite the ambiguous and challenging nature of the data, GEM still obtain commendable disentanglement outcomes, affirming its robustness.

4.4 Evaluations of MLLMs

Before utilizing the interrelation discovery branch, it is imperative to investigate the reliability of MLLMs. This evaluation guarantees that the identified interrelations and their associated impact scores are dependable and can be effectively applied to downstream modules. To this purpose, we evaluate three latest MLLMs including GPT-4o, GPT-4v and GLM-4—against the ground truth attributes of the CelebA dataset. The horizontal axis presents the targeted attributes selected from the CelebA, where the vertical axis presents the percentage of scoring accuracy.

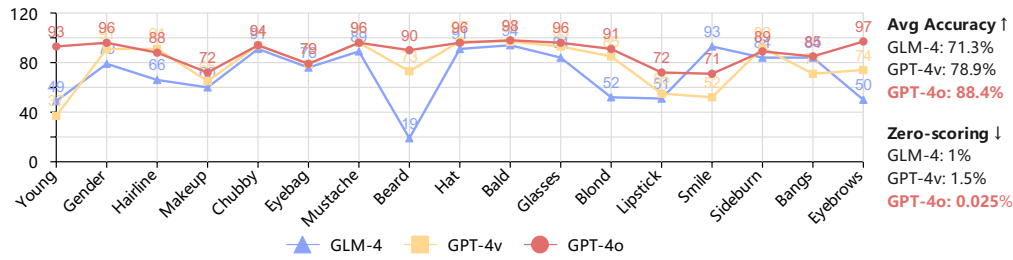


Figure 6: Evaluation experiments on the various MLLMs for attributes scoring.

As reported in Figure 6, GPT-4o outperforms other models on individual attribute scoring, achieving accuracy exceeding 90% for the majority of attributes. Specifically, it exhibits superior performance on attributes like *Beard*, *Young*, and *Eyebrows*, where other models yield significantly lower scores. In addition, GPT-4o achieves the highest average accuracy of 88.4% and the lowest zero-scoring rate at 0.025%, indicating a minimal rate of the meaningless predictions where all attributes are scored as zero. Based on the evaluations, we employ GPT-4o as the interrelation predictor in the model.

4.5 Ablation Study

To analyze the effectiveness of individual components in GEM, we perform an ablation study focusing on the importance of the β -VAE based branch, GNN-based graph learner E_{gnn} , and adversarial training strategy. The CelebA dataset served as the experimental platform for the investigations. It is worth noting that the complete removal of β -VAE branch is infeasible, as it would prevent the model from extracting attributes. Therefore to evaluate the importance of independent attribute extraction, we replace the β -VAE with the vanilla VAE, which does not enforce the independence of factors.

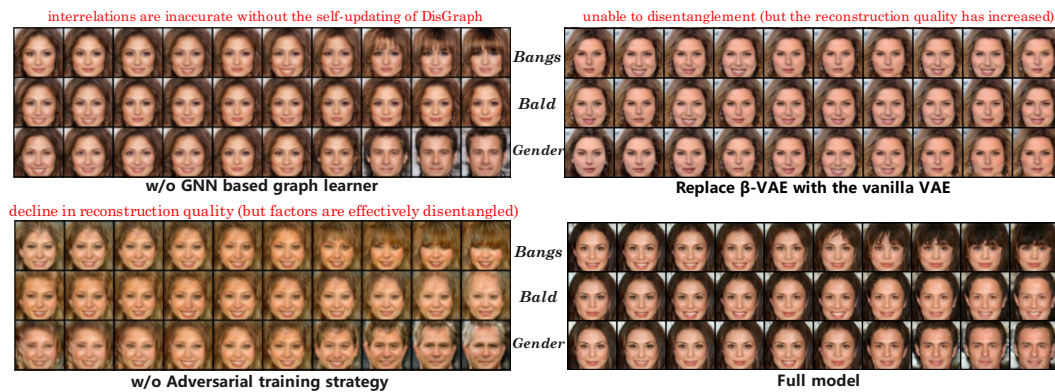


Figure 7: Ablation on replacing β -VAE with VAE, w/o graph learner, and w/o adversarial strategy.

As depicted in Figure 7, replacing β -VAE encoder results in a declined disentanglement capability, albeit with an improvement in reconstruction quality. In addition, the removal of GNN-based graph learner prevents the parameter updating of DisGraph, leading to the inaccurate determination of relations (e.g., the relation between *Bald* and *Gender* weakens). It is worth noting that the removal of both graph learner and initialization process within the framework precludes the learning of interrelations. Furthermore, eliminating the adversarial training strategy in GEM and relying solely on the standard VAE loss function results in a significant decline in reconstruction quality. The aforementioned results highlight the effectiveness of each part of our framework.

5 Conclusion

In this paper, we aim to explore the logical interrelations between semantic attributes within complex data, which is a critical challenge that existing DRL have yet to properly address. To this end, we introduce GEM, a β -VAE and MLLMs-based framework, designed to achieve fine-grained and relation-aware disentanglement. In this framework, DRL and MLLMs are integrated via a bidirectional and self-driven graph. Both qualitative and quantitative experiments demonstrate GEM’s superior disentanglement and reconstruction capacities over typical DRL models. In addition, the model shows its enhanced interpretability and generalizability inherited from MLLMs.

References

- [1] Yoshua Bengio, Aaron Courville, and Pascal Vincent. Representation learning: A review and new perspectives. *IEEE transactions on pattern analysis and machine intelligence*, 35(8):1798–1828, 2013.
- [2] Luan Tran, Xi Yin, and Xiaoming Liu. Disentangled representation learning gan for pose-invariant face recognition. In *Proceedings of the IEEE conference on computer vision and pattern recognition*, pages 1415–1424, 2017.
- [3] Mingi Kwon, Jaeseok Jeong, and Youngjung Uh. Diffusion models already have a semantic latent space. *arXiv preprint arXiv:2210.10960*, 2022.
- [4] Abhishek Kumar, Prasanna Sattigeri, and Avinash Balakrishnan. Variational inference of disentangled latent concepts from unlabeled observations. *arXiv preprint arXiv:1711.00848*, 2017.
- [5] Andrey Voynov and Artem Babenko. Unsupervised discovery of interpretable directions in the gan latent space. In *International conference on machine learning*, pages 9786–9796. PMLR, 2020.
- [6] Pengyu Cheng, Martin Renqiang Min, Dinghan Shen, Christopher Malon, Yizhe Zhang, Yitong Li, and Lawrence Carin. Improving disentangled text representation learning with information-theoretic guidance. *arXiv preprint arXiv:2006.00693*, 2020.
- [7] Zhenya Huang, Xin Lin, Hao Wang, Qi Liu, Enhong Chen, Jianhui Ma, Yu Su, and Wei Tong. Disenqnet: Disentangled representation learning for educational questions. In *Proceedings of the 27th ACM SIGKDD Conference on Knowledge Discovery & Data Mining*, pages 696–704, 2021.
- [8] Giangiacomo Mercatali and André Freitas. Disentangling generative factors in natural language with discrete variational autoencoders. *arXiv preprint arXiv:2109.07169*, 2021.
- [9] Xi Chen, Yan Duan, Rein Houthoofd, John Schulman, Ilya Sutskever, and Pieter Abbeel. Infogan: Interpretable representation learning by information maximizing generative adversarial nets. *Advances in neural information processing systems*, 29, 2016.
- [10] Hong Chen, Yipeng Zhang, Xin Wang, Xuguang Duan, Yuwei Zhou, and Wenwu Zhu. Disenbooth: Disentangled parameter-efficient tuning for subject-driven text-to-image generation. *arXiv preprint arXiv:2305.03374*, 2023.
- [11] Krishna Kumar Singh, Utkarsh Ojha, and Yong Jae Lee. Finegan: Unsupervised hierarchical disentanglement for fine-grained object generation and discovery. In *Proceedings of the IEEE/CVF conference on computer vision and pattern recognition*, pages 6490–6499, 2019.
- [12] Diederik P Kingma and Max Welling. Auto-encoding variational bayes. *arXiv preprint arXiv:1312.6114*, 2013.
- [13] Irina Higgins, Loic Matthey, Arka Pal, Christopher P Burgess, Xavier Glorot, Matthew M Botvinick, Shakir Mohamed, and Alexander Lerchner. beta-vae: Learning basic visual concepts with a constrained variational framework. *ICLR (Poster)*, 3, 2017.
- [14] Ricky TQ Chen, Xuechen Li, Roger B Grosse, and David K Duvenaud. Isolating sources of disentanglement in variational autoencoders. *Advances in neural information processing systems*, 31, 2018.
- [15] Christopher P Burgess, Irina Higgins, Arka Pal, Loic Matthey, Nick Watters, Guillaume Desjardins, and Alexander Lerchner. Understanding disentangling in β -vae. *arXiv preprint arXiv:1804.03599*, 2018.
- [16] Cristian Meo, Louis Mahon, Anirudh Goyal, and Justin Dauwels. β -tc-vae: On the relationship between disentanglement and diversity. In *The Twelfth International Conference on Learning Representations*, 2023.
- [17] Xin Wang, Hong Chen, Si’ao Tang, Zihao Wu, and Wenwu Zhu. Disentangled representation learning. *arXiv preprint arXiv:2211.11695*, 2022.
- [18] Francesco Locatello, Stefan Bauer, Mario Lucic, Gunnar Raetsch, Sylvain Gelly, Bernhard Schölkopf, and Olivier Bachem. Challenging common assumptions in the unsupervised learning of disentangled representations. In *international conference on machine learning*, pages 4114–4124. PMLR, 2019.
- [19] Mengyue Yang, Furuo Liu, Zhitang Chen, Xinwei Shen, Jianye Hao, and Jun Wang. Causalvae: Disentangled representation learning via neural structural causal models. In *Proceedings of the IEEE/CVF conference on computer vision and pattern recognition*, pages 9593–9602, 2021.
- [20] Xingyi Yang, Jingwen Ye, and Xinchao Wang. Factorizing knowledge in neural networks. In *European Conference on Computer Vision*, pages 73–91. Springer, 2022.
- [21] Saeed Amizadeh, Hamid Palangi, Alex Polozov, Yichen Huang, and Kazuhito Koishida. Neuro-symbolic visual reasoning: Disentangling. In *International Conference on Machine Learning*, pages 279–290. Pmlr, 2020.
- [22] Tameem Adel, Han Zhao, and Richard E Turner. Continual learning with adaptive weights (claw). *arXiv preprint arXiv:1911.09514*, 2019.

- [23] Zhiyuan Li, Jaideep Vitthal Murkute, Prashna Kumar Gyawali, and Linwei Wang. Progressive learning and disentanglement of hierarchical representations. *arXiv preprint arXiv:2002.10549*, 2020.
- [24] Bin Tong, Chao Wang, Martin Klinkigt, Yoshiyuki Kobayashi, and Yuuichi Nonaka. Hierarchical disentanglement of discriminative latent features for zero-shot learning. In *Proceedings of the IEEE/CVF conference on computer vision and pattern recognition*, pages 11467–11476, 2019.
- [25] Pengzhou Wu and Kenji Fukumizu. β -intact-vae: Identifying and estimating causal effects under limited overlap. *arXiv preprint arXiv:2110.05225*, 2021.
- [26] Di Fan, Yannian Kou, and Chuanhou Gao. Causal disentangled representation learning with vae and causal flows. *Journal of Machine Learning Research*, 2022.
- [27] Xinwei Shen, Furui Liu, Hanze Dong, Qing Lian, Zhitang Chen, and Tong Zhang. Weakly supervised disentangled generative causal representation learning. *Journal of Machine Learning Research*, 23(241):1–55, 2022.
- [28] Insu Jeon, Wonkwang Lee, Myeongjang Pyeon, and Gunhee Kim. Ib-gan: Disentangled representation learning with information bottleneck generative adversarial networks. In *Proceedings of the AAAI Conference on Artificial Intelligence*, volume 35, pages 7926–7934, 2021.
- [29] Tao Yang, Yuwang Wang, Cuiling Lan, Yan Lu, and Nanning Zheng. Vector-based representation is the key: A study on disentanglement and compositional generalization. *arXiv preprint arXiv:2305.18063*, 2023.
- [30] Xin Jin, Bohan Li, Baao Xie, Wenyao Zhang, Jinming Liu, Ziqiang Li, Tao Yang, and Wenjun Zeng. Closed-loop unsupervised representation disentanglement with β -vae distillation and diffusion probabilistic feedback. *arXiv preprint arXiv:2402.02346*, 2024.
- [31] Agisilaos Chartsias, Thomas Joyce, Giorgos Papanastasiou, Scott Semple, Michelle Williams, David E Newby, Rohan Dharmakumar, and Sotirios A Tsaftaris. Disentangled representation learning in cardiac image analysis. *Medical image analysis*, 58:101535, 2019.
- [32] Cosmin I Bercea, Benedikt Wiestler, Daniel Rueckert, and Shadi Albarqouni. Federated disentangled representation learning for unsupervised brain anomaly detection. *Nature Machine Intelligence*, 4(8):685–695, 2022.
- [33] Lianrui Zuo, Yihao Liu, Jerry L Prince, and Aaron Carass. An overview of disentangled representation learning for mr image harmonization. *Deep Learning for Medical Image Analysis*, pages 135–152, 2024.
- [34] Abel Gonzalez-Garcia, Joost Van De Weijer, and Yoshua Bengio. Image-to-image translation for cross-domain disentanglement. *Advances in neural information processing systems*, 31, 2018.
- [35] Hsin-Ying Lee, Hung-Yu Tseng, Jia-Bin Huang, Maneesh Singh, and Ming-Hsuan Yang. Diverse image-to-image translation via disentangled representations. In *Proceedings of the European conference on computer vision (ECCV)*, pages 35–51, 2018.
- [36] Boqiang Zhang, Hongtao Xie, Zuan Gao, and Yuxin Wang. Choose what you need: Disentangled representation learning for scene text recognition, removal and editing. *arXiv preprint arXiv:2405.04377*, 2024.
- [37] Piaopiao Yu, Jie Guo, Fan Huang, Cheng Zhou, Hongwei Che, Xiao Ling, and Yanwen Guo. Hierarchical disentangled representation learning for outdoor illumination estimation and editing. In *Proceedings of the IEEE/CVF International Conference on Computer Vision*, pages 15313–15322, 2021.
- [38] Baao Xie, Bohan Li, Zequn Zhang, Junting Dong, Xin Jin, Jingyu Yang, and Wenjun Zeng. Navinerf: Nerf-based 3d representation disentanglement by latent semantic navigation. In *Proceedings of the IEEE/CVF International Conference on Computer Vision*, pages 17992–18002, 2023.
- [39] Katja Schwarz, Yiyi Liao, Michael Niemeyer, and Andreas Geiger. Graf: Generative radiance fields for 3d-aware image synthesis. *Advances in Neural Information Processing Systems*, 33:20154–20166, 2020.
- [40] Michael Niemeyer and Andreas Geiger. Giraffe: Representing scenes as compositional generative neural feature fields. In *Proceedings of the IEEE/CVF Conference on Computer Vision and Pattern Recognition*, pages 11453–11464, 2021.
- [41] Hyunjik Kim and Andriy Mnih. Disentangling by factorising. In *International conference on machine learning*, pages 2649–2658. PMLR, 2018.
- [42] Minyoung Kim, Yuting Wang, Pritish Sahu, and Vladimir Pavlovic. Relevance factor vae: Learning and identifying disentangled factors. *arXiv preprint arXiv:1902.01568*, 2019.
- [43] Zihao Chen, Wenyong Wang, and Sai Zou. Break the spell of total correlation in betatcvae. *arXiv preprint arXiv:2210.08794*, 2022.
- [44] Karsten Roth, Mark Ibrahim, Zeynep Akata, Pascal Vincent, and Diane Bouchacourt. Disentanglement of correlated factors via hausdorff factorized support. *arXiv preprint arXiv:2210.07347*, 2022.

- [45] Yunhao Ge, Sami Abu-El-Haija, Gan Xin, and Laurent Itti. Zero-shot synthesis with group-supervised learning. *arXiv preprint arXiv:2009.06586*, 2020.
- [46] Matthew J Vowels, Necati Cihan Camgoz, and Richard Bowden. Gated variational autoencoders: Incorporating weak supervision to encourage disentanglement. In *2020 15th IEEE International Conference on Automatic Face and Gesture Recognition (FG 2020)*, pages 125–132. IEEE, 2020.
- [47] Diane Bouchacourt, Ryota Tomioka, and Sebastian Nowozin. Multi-level variational autoencoder: Learning disentangled representations from grouped observations. In *Proceedings of the AAAI Conference on Artificial Intelligence*, volume 32, 2018.
- [48] Attila Szabo, Qiyang Hu, Tiziano Portenier, Matthias Zwicker, and Paolo Favaro. Understanding degeneracies and ambiguities in attribute transfer. In *Proceedings of the European Conference on Computer Vision (ECCV)*, pages 700–714, 2018.
- [49] Andrew Ross and Finale Doshi-Velez. Benchmarks, algorithms, and metrics for hierarchical disentanglement. In *International Conference on Machine Learning*, pages 9084–9094. PMLR, 2021.
- [50] Xinyang Li, Shengchuan Zhang, Jie Hu, Liujuan Cao, Xiaopeng Hong, Xudong Mao, Feiyue Huang, Yongjian Wu, and Rongrong Ji. Image-to-image translation via hierarchical style disentanglement. In *Proceedings of the IEEE/CVF conference on computer vision and pattern recognition*, pages 8639–8648, 2021.
- [51] Wayne Xin Zhao, Kun Zhou, Junyi Li, Tianyi Tang, Xiaolei Wang, Yupeng Hou, Yingqian Min, Beichen Zhang, Junjie Zhang, Zican Dong, et al. A survey of large language models. *arXiv preprint arXiv:2303.18223*, 2023.
- [52] Alec Radford, Jong Wook Kim, Chris Hallacy, Aditya Ramesh, Gabriel Goh, Sandhini Agarwal, Girish Sastry, Amanda Askell, Pamela Mishkin, Jack Clark, et al. Learning transferable visual models from natural language supervision. In *International conference on machine learning*, pages 8748–8763. PMLR, 2021.
- [53] Bin Lin, Zhenyu Tang, Yang Ye, Jiayi Cui, Bin Zhu, Peng Jin, Junwu Zhang, Munan Ning, and Li Yuan. Moe-llava: Mixture of experts for large vision-language models. *arXiv preprint arXiv:2401.15947*, 2024.
- [54] Yuliang Liu, Biao Yang, Qiang Liu, Zhang Li, Zhiyin Ma, Shuo Zhang, and Xiang Bai. Textmonkey: An ocr-free large multimodal model for understanding document. *arXiv preprint arXiv:2403.04473*, 2024.
- [55] R OpenAI. Gpt-4 technical report. arxiv 2303.08774. *View in Article*, 2(5), 2023.
- [56] Gemini Team, Rohan Anil, Sebastian Borgeaud, Yonghui Wu, Jean-Baptiste Alayrac, Jiahui Yu, Radu Soricut, Johan Schalkwyk, Andrew M Dai, Anja Hauth, et al. Gemini: a family of highly capable multimodal models. *arXiv preprint arXiv:2312.11805*, 2023.
- [57] Yossi Gandelsman, Alexei A Efros, and Jacob Steinhardt. Interpreting clip’s image representation via text-based decomposition. *arXiv preprint arXiv:2310.05916*, 2023.
- [58] Zhengyuan Yang, Linjie Li, Kevin Lin, Jianfeng Wang, Chung-Ching Lin, Zicheng Liu, and Lijuan Wang. The dawn of llms: preliminary explorations with gpt-4v (ision). arxiv. *arXiv preprint arXiv:2309.17421*, 2023.
- [59] OpenAI. Gpt-4v(ision) system card. *arXiv preprint*, 2023.
- [60] OpenAI. Hello, gpt-4o. *OpenAI*, 2025.
- [61] Maxim Enis and Mark Hopkins. From llm to nmt: Advancing low-resource machine translation with claude. *arXiv preprint arXiv:2404.13813*, 2024.
- [62] Shengqiong Wu, Hao Fei, Leigang Qu, Wei Ji, and Tat-Seng Chua. Next-gpt: Any-to-any multimodal llm. *arXiv preprint arXiv:2309.05519*, 2023.
- [63] Angus Yang, Zehan Li, and Jie Li. Advancing genai assisted programming—a comparative study on prompt efficiency and code quality between gpt-4 and glm-4. *arXiv preprint arXiv:2402.12782*, 2024.
- [64] Samyadeep Basu, Keivan Rezaei, Ryan Rossi, Cherry Zhao, Vlad Morariu, Varun Manjunatha, and Soheil Feizi. On mechanistic knowledge localization in text-to-image generative models. *arXiv preprint arXiv:2405.01008*, 2024.
- [65] Harshvardhan Sikka, Weishun Zhong, Jun Yin, and Cengiz Pehlevant. A closer look at disentangling in β -vae. In *2019 53rd Asilomar Conference on Signals, Systems, and Computers*, pages 888–895. IEEE, 2019.
- [66] Deokyun Kim, Minseon Kim, Gihyun Kwon, and Dae-Shik Kim. Progressive face super-resolution via attention to facial landmark. *arXiv preprint arXiv:1908.08239*, 2019.
- [67] Giuseppe Amato, Fabrizio Falchi, Claudio Gennaro, and Claudio Vairo. A comparison of face verification with facial landmarks and deep features. In *10th International Conference on Advances in Multimedia (MMEDIA)*, pages 1–6, 2018.

- [68] Martin Heusel, Hubert Ramsauer, Thomas Unterthiner, Bernhard Nessler, and Sepp Hochreiter. Gans trained by a two time-scale update rule converge to a local nash equilibrium. *Advances in neural information processing systems*, 30, 2017.
- [69] Robert H Somers. A new asymmetric measure of association for ordinal variables. *American sociological review*, pages 799–811, 1962.
- [70] Maurice G Kendall. A new measure of rank correlation. *Biometrika*, 30(1/2):81–93, 1938.
- [71] Yixin Liu, Yu Zheng, Daokun Zhang, Hongxu Chen, Hao Peng, and Shirui Pan. Towards unsupervised deep graph structure learning. In *Proceedings of the ACM Web Conference 2022*, pages 1392–1403, 2022.
- [72] Thomas N Kipf and Max Welling. Semi-supervised classification with graph convolutional networks. *arXiv preprint arXiv:1609.02907*, 2016.
- [73] Ziwei Liu, Ping Luo, Xiaogang Wang, and Xiaoou Tang. Deep learning face attributes in the wild. In *Proceedings of International Conference on Computer Vision (ICCV)*, December 2015.
- [74] Fisher Yu, Ari Seff, Yinda Zhang, Shuran Song, Thomas Funkhouser, and Jianxiong Xiao. Lsun: Construction of a large-scale image dataset using deep learning with humans in the loop. *arXiv preprint arXiv:1506.03365*, 2015.
- [75] Adam Paszke, Sam Gross, Soumith Chintala, Gregory Chanan, Edward Yang, Zachary DeVito, Zeming Lin, Alban Desmaison, Luca Antiga, and Adam Lerer. Automatic differentiation in pytorch. *Online*, 2017.
- [76] Jonathan Ho, Ajay Jain, and Pieter Abbeel. Denoising diffusion probabilistic models. *Advances in neural information processing systems*, 33:6840–6851, 2020.